Letter

Simple formulas of directional amplification from non-Bloch band theory

Wen-Tan Xue, Ming-Rui Li, Yu-Min Hu, Fei Song, and Zhong Wang*
Institute for Advanced Study, Tsinghua University, Beijing 100084, China

(Received 10 May 2020; revised 23 May 2021; accepted 28 May 2021; published 15 June 2021)

Green's functions are fundamental quantities that determine the linear responses of physical systems. The recent developments of non-Hermitian systems, therefore, call for Green's function formulas of non-Hermitian bands. This task is complicated by the high sensitivity of energy spectrums to boundary conditions, which invalidates the straightforward generalization of Hermitian formulas. Here, based on the non-Bloch band theory, we obtain simple Green's function formulas of general one-dimensional non-Hermitian bands. Furthermore, in the large-size limit, these formulas dramatically reduce to finding the roots of a simple algebraic equation. As an application, our formulation provides the desirable formulas for the defining quantities, the gain and directionality, of directional amplification. Thus our formulas provide an efficient guide for designing directional amplifiers.

DOI: 10.1103/PhysRevB.103.L241408

The responses of a physical system are generally proportional to a sufficiently weak perturbation, which is captured by the Green's functions. Whereas their explicit formulas are well known for Hermitian energy bands, recent progresses in non-Hermitian systems call for their generalizations. This seemingly straightforward task is hindered by the non-Hermitian skin effect [1–7], meaning the exponential localization of most eigenstates to the boundaries. This effect causes a high sensitivity of Green's functions to the boundary condition, invalidating a straightforward extension of Hermitian formulas. It is the purpose of this Letter to obtain general formulas of non-Hermitian Green's functions.

The problem can be simply phrased. Let us consider a general non-Hermitian Hamiltonian H of one-dimensional (1D) lattice with length L, with translational symmetry $H_{ij} = H_{i+1,j+1}$ (for $i, j = 1, 2, \ldots, L-1$). For example, if we take $H_{i,i\pm1} = t_1, H_{i,i\pm2} = t_2 \mp \gamma/2, H_{ii} = i\kappa$ and all other matrix elements zero, H can be shown pictorially as Fig. 1(a). We take an open-boundary condition (OBC) at the two ends [8]. Our goal is to find explicit formulas for the frequency-domain Green's function matrix

$$G(\omega) = \frac{1}{\omega - H}. \tag{1}$$

Although Green's functions have recently been studied to extract non-Hermitian topology [9–11], their general and explicit formulas have been lacking. As we will see, this seemingly trivial goal is difficult, if not impossible, to achieve from the standard Brillouin zone (BZ) and Bloch-band framework. Here, we will obtain the G matrix from the non-Bloch band theory [1,12], which is based on the generalized Brillouin zone (GBZ) originally introduced to understand non-Hermitian topology [1,3,12–24]. We obtain a simple integral formula for all the matrix elements $G_{ij}(\omega)$. In particular, for the end-to-end Green's functions, G_{L1} and G_{1L}, our integral formula reduces in the large-L limit to

$$G_{L1}(\omega) \sim [\beta_M(\omega)]^L, \quad G_{1L}(\omega) \sim [\beta_{M+1}(\omega)]^{-L}, \tag{2}$$

where $\beta_{j=1,\ldots,2M}$ are the roots of $h(\beta) = \omega$ ordered as $|\beta_1| \leqslant \cdots \leqslant |\beta_{2M}|$. Here, $h(\beta)$ denotes the Bloch Hamiltonian of H, under the notation $\beta \equiv e^{ik}$, which takes the general form of $h(\beta) = \sum_{n=-M}^{M} h_n \beta^n$ with coefficients $h_n = H_{i,i+n}$, with M being the hopping range. For example, for the model Fig. 1(a), we have $M = 2$ and

$$h(\beta) = \left(t_2 + \frac{\gamma}{2}\right)\beta^{-2} + t_1\beta^{-1} + i\kappa + t_1\beta + \left(t_2 - \frac{\gamma}{2}\right)\beta^2. \tag{3}$$

As we will show, the presence in Eq. (2) of the *middle two* roots, namely the Mth and $(M+1)$th of the $2M$ roots, reflects the GBZ origin of Eq. (2).

Among various applications, our formulas are important for directional amplifiers (or nonreciprocal amplifiers). In such devices, signals are amplified in a preferred direction and suppressed in the reversed direction, which protects the signal sources; such a feature is essential to a wide range of applications in classical and quantum information processing [25–42]. Irrespective of device details, their dynamics is generated by effective non-Hermitian Hamiltonians [36–50], and the gain and directionality are given by the Green's function [36,37,43]. To be precise, directional amplification occurs when $|G_{ij}(\omega)| \gg 1$ while $|G_{ji}(\omega)| \ll 1$ for a certain pair (i, j), meaning that an ω-frequency signal is amplified from j to i, while the back-propagation from i to j is suppressed. Although brute force calculation of the Green's function is viable for few-mode cases, it becomes inconvenient for many-mode amplifiers taking the shape of a 1D chain; such 1D amplifiers have the advantage of unlimited gain-bandwidth product without fine-tuning [46,47]. Our Green's function formulas tell their gain and directionality in a simple fashion.

Integral formulas of Green's function. Numerically, $G_{ij}(\omega)$ follows an exponential law with respect to $|i-j|$. For

*wangzhongemail@gmail.com

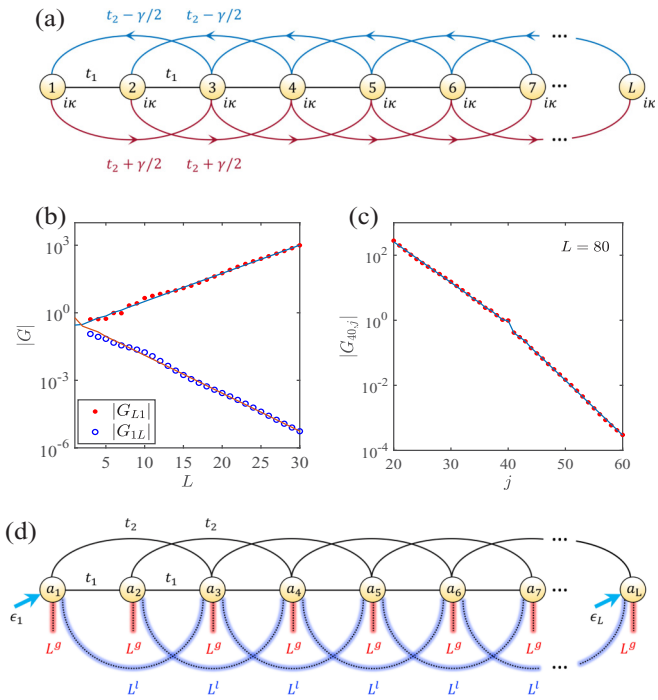

FIG. 1. (a) Hamiltonian H, with open-boundary condition (OBC) at the two ends. (b) $|G_{L1}|$ and $|G_{1L}|$. The corresponding curve represents Eq. (9) and Eq. (10), with $|K| = 0.292$ and 0.619, respectively. (c) $|G_{40,j}|$ for $L = 80$ (dots). Blue curve represents Eq. (8). For (b) and (c), parameters are $t_1 = t_2 = 1$, $\gamma = 4/3$, $\kappa = -0.8$, and $\omega = -1.7$. (d) An open quantum system whose effective Hamiltonian is (a). Gain and loss are denoted by $L^{g,l}$ and the external signals by ϵ_i.

example, the end-to-end Green's functions for our specific model [Fig. 1(a)] have the following large-L behaviors:

$$|G_{L1}(\omega)| \sim (\alpha_{\rightarrow})^L, \quad |G_{1L}(\omega)| \sim (\alpha_{\leftarrow})^L, \tag{4}$$

which are displayed in Fig. 1(b). Knowing $\alpha_{\rightarrow}$ and $\alpha_{\leftarrow}$ is important to understanding and designing directional amplification. The condition for rightward amplification, $|G_{L1}| \gg 1$ and $|G_{1L}| \ll 1$, is to require $\alpha_{\rightarrow} > 1$ and $\alpha_{\leftarrow} < 1$; similarly, the condition for leftward amplification is to require $\alpha_{\rightarrow} < 1, \alpha_{\leftarrow} > 1$. Remarkably, such 1D amplification does not suffer from the standard limitation of gain-bandwidth product, because large gain is possible for large L, while the bandwidth is independent of L [46,47].

The values of $\alpha_{\rightarrow}$ and $\alpha_{\leftarrow}$ can be derived from the general formulas of $G_{ij}(\omega)$ to be obtained below. To derive the general $G_{ij}(\omega)$, a plausible starting point is the spectral representation $(\omega - H)^{-1} = \sum_n (\omega - E_n)^{-1} |\psi_{nR}\rangle\langle\psi_{nL}|$, where E_n and $|\psi_{nR(L)}\rangle$ are the eigenvalues and normalized right (left) eigenvectors of H under OBC, namely, $H|\psi_{nR}\rangle = E_n|\psi_{nR}\rangle$, $\langle\psi_{nL}|H = \langle\psi_{nL}|E_n$. Moreover, it is tempting to switch to the BZ and conjecture that

$$G_{ij}(\omega) = \int_0^{2\pi} \frac{dk}{2\pi} \frac{e^{ik(i-j)}}{\omega - h(k)}. \tag{5}$$

With the notation $\beta = e^{ik}$, BZ is the unit circle and the integral becomes

$$G_{ij}(\omega) = \int_{|\beta|=1} \frac{d\beta}{2\pi i\beta} \frac{\beta^{i-j}}{\omega - h(\beta)}. \tag{6}$$

An immediate difficulty is seen after using the residue theorem, which leads to $G_{L1} \sim (\beta_a)^L$, with β_a being the largest-modulus root of $\omega - h(\beta) = 0$ inside the unit circle. This would always imply $\alpha_{\rightarrow} = |\beta_a| < 1$ and forbids any directional amplification. Similarly, one would have $\alpha_{\leftarrow} = 1/|\beta_{a'}| < 1$, with $\beta_{a'}$ being the smallest-modulus root outside the unit circle. In fact, Eq. (6) is generally valid only in Hermitian cases, as will become clear below.

The problem with Eq. (6) is the assumption of the validity of Bloch band theory. In fact, a unique non-Hermitian phenomenon is that, for a broad class of non-Hermitian Hamiltonians, all the eigenstates are localized at the boundaries, which is known as the non-Hermitian skin effect [1–7]. This effect suggests that we should remove the usual Bloch-band restriction $|\beta| = 1$. Indeed, it has been found that when β varies in a closed curve known as the GBZ in the complex plane, the trajectory of $h(\beta)$ is exactly the OBC energy band [1,12]. Note that, if β varies in the BZ ($|\beta| = 1$), the $h(\beta)$ trajectory is the periodic-boundary-condition (PBC) energy band, which is generally different from the OBC energy band. In Hermitian cases, GBZ reduces to the BZ, being consistent with the fact that PBC and OBC bands are the same. The equation that determines the GBZ was found in Refs. [1,12]; we recall their final result below without reproducing the technical derivations. For a hopping range M, $h(\beta) = E$ is a $2M$th order equation with roots $\beta_1(E), \beta_2(E), \ldots, \beta_{2M}(E)$, which are ordered as $|\beta_1| \leqslant |\beta_2| \leqslant \cdots \leqslant |\beta_{2M}|$. The GBZ equation reads [1,12]

$$|\beta_M(E)| = |\beta_{M+1}(E)|, \tag{7}$$

which is essentially a single-variable equation because β_M, β_{M+1}, E are related by $h(\beta_M) = h(\beta_{M+1}) = E$. The β_M and β_{M+1} solutions form a closed loop in the complex plane, which is the GBZ, and the E solutions form the OBC energy bands. Examples of GBZ are shown in Figs. 2(a) and 2(e).

In view of the failure of BZ [e.g., invalidity of Eq. (6)], we propose the following GBZ-based integral formula for G_{ij}:

$$G_{ij}(\omega) = \int_{\mathrm{GBZ}} \frac{d\beta}{2\pi i\beta} \frac{\beta^{i-j}}{\omega - h(\beta)}, \tag{8}$$

which is a main result of this Letter. Its proof is provided in the Supplemental Material [53]. In practice, this integral is highly convenient to evaluate by the residue theorem, which reduces it to a sum at several roots of $h(\beta) = \omega$. This simplification is enabled by the vital fact that the GBZ is always a closed loop [1,12,15]. A numerical confirmation of Eq. (8) is shown in Fig. 1(c). Irrespective of $|i - j|$ being large or small, the formula is always precise for i, j not too close to the two ends. At the two ends, because of the boundary effect, a factor K of order unity has to be included:

$$G_{L1}(\omega) = K \int_{\mathrm{GBZ}} \frac{d\beta}{2\pi i\beta} \frac{\beta^{L-1}}{\omega - h(\beta)}, \tag{9}$$

$$G_{1L}(\omega) = K \int_{\mathrm{GBZ}} \frac{d\beta}{2\pi i\beta} \frac{\beta^{-(L-1)}}{\omega - h(\beta)}. \tag{10}$$

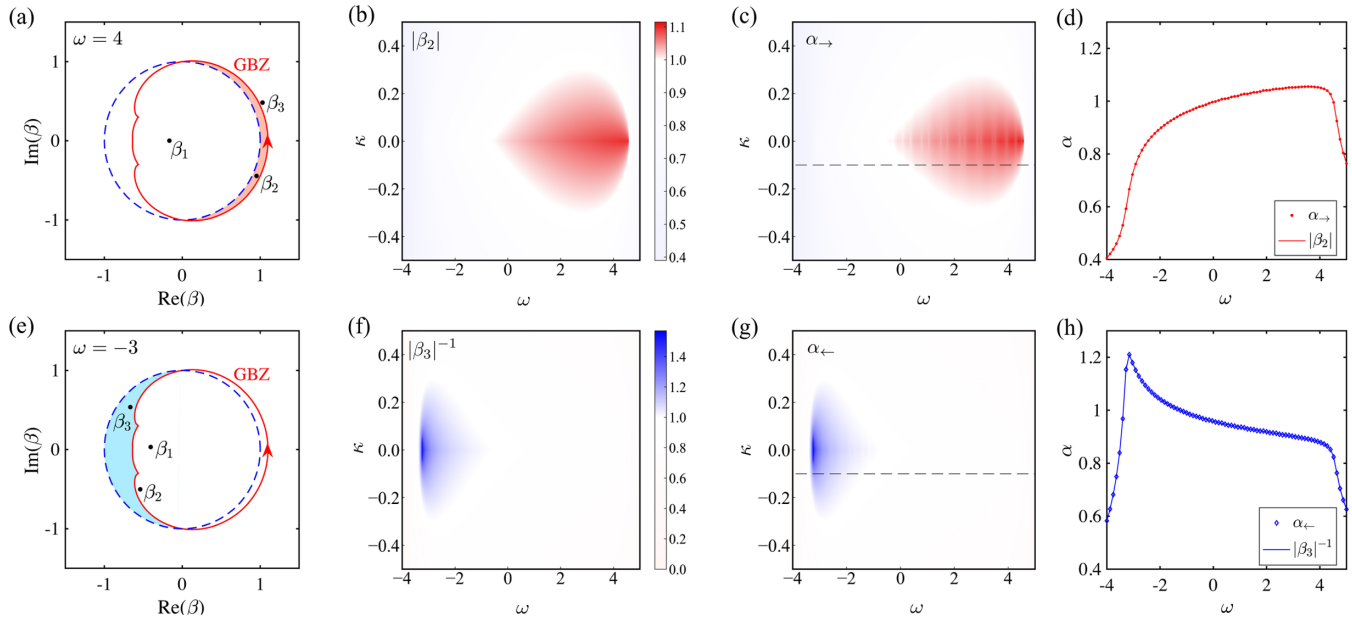

FIG. 2. (a) GBZ (red solid loop) and BZ (blue dashed circle). $\beta_{1,2,3}$ are roots of $h(\beta) = \omega$ for $\kappa = -0.1$ and $\omega = 4$ (β_4 is outside this region). When there exists a root in the colored region inside GBZ but outside BZ, rightward amplification occurs. (b) $|\beta_2|$ as a function of κ, ω. (c) $\alpha_\rightarrow$ from Eq. (4). (d) $\alpha_\rightarrow$ and $|\beta_2|$ along the cut $\kappa = -0.1$ [dashed line in (c)]. (e) The same as (a) except that $\omega = -3$. When there exists a root in the colored region inside BZ but outside GBZ, leftward amplification occurs. (f) $|\beta_3|^{-1}$. (g) $\alpha_\leftarrow$. (h) $\alpha_\leftarrow$ and $|\beta_3|^{-1}$ along the cut $\kappa = -0.1$. Parameter values are $t_1 = 2$, $t_2 = 0.3$, and $\gamma = 0.3$.

Now Eq. (2) can be derived as follows. Ordering the roots of $h(\beta) = \omega$ as $|\beta_1| \leqslant |\beta_2| \leqslant \cdots \leqslant |\beta_{2M}|$, one can prove that $\beta_1, \ldots, \beta_M$ are enclosed by the GBZ, while $\beta_{M+1}, \ldots, \beta_{2M}$ are not. To see this, suppose that we vary ω in the complex plane (though ω is real valued for physical applications). As long as ω stays away from the OBC energy spectrum $E_{\rm OBC}$, the roots β_i's cannot touch the GBZ because GBZ generates $E_{\rm OBC}$. Therefore, the number of roots enclosed by GBZ is independent of ω. To determine this number, we consider the $|\omega| \to \infty$ limit, in which either the β^M or β^{-M} term dominates $h(\beta)$ and there are M roots with $|\beta| \sim |\omega|^{1/M} \to \infty$, and also M roots with $|\beta| \sim |\omega|^{-1/M} \to 0$. Therefore, for any ω, there are M roots $\beta_{1,2,\ldots,M}$ inside the GBZ (for a more rigorous proof, see Refs. [51,52]). Now Eq. (9) and Eq. (10) can be simplified by the residue theorem. For large L, we obtain Eq. (2); in other words,

$$\alpha_\rightarrow = |\beta_M(\omega)|, \quad \alpha_\leftarrow = |\beta_{M+1}(\omega)|^{-1}. \tag{11}$$

Therefore, the *middle two* roots of $h(\beta) = \omega$, β_M and β_{M+1}, determine the gain and directionality, leading to a surprising simplification. The indices M and $M+1$ are difficult to understand from the BZ; they reflect the GBZ origin of Eqs. (2) and (11). Equations (8)–(11) are the central results of this work. For multiband systems, $h(\beta)$ is a matrix, and Eq. (11) remains applicable with $\beta_{j=1,\ldots,2M}$ denoting the roots of $\det[\omega - h(\beta)] = 0$ (see Supplemental Material [53]).

As an application to the model in Fig. 1(a), we show in Fig. 2 a quantitative comparison of our theory with the extensive numerical results. For all the parameters investigated, the numerical $\alpha_\rightarrow$ and $\alpha_\leftarrow$ are in excellent agreement with Eq. (11) with $M = 2$. Pictorially, rightward and leftward amplification occurs when a root locates in the colored area in Figs. 2(a) and 2(e), respectively. Notably, the amplifier can selectively amplify signals in a frequency-dependent direction. In our theory, this frequency-dependent directionality is possible when the GBZ has intersections with the BZ [Figs. 2(a) and 2(e)]. This picture provides a mechanism for designing devices that efficiently integrate directional amplifiers and frequency filters or splitters. On the other hand, the simpler cases of rightward (leftward) unidirectional amplification within the entire bandwidth are realized when the GBZ is entirely outside (inside) the BZ (an example is shown in the Supplemental Material [53]).

Intuitively, the nonreciprocal hoppings seem to favor motion towards a preferred direction, causing directional amplification in that direction; e.g., when $|t_2 + \gamma/2| > |t_2 - \gamma/2|$ in Fig. 1(a), it seems that the directional amplification should be rightward. However, as has been shown above, leftward directional amplification is also seen in certain frequency windows. Thus the simple intuition based on hopping direction fails even qualitatively by telling a wrong amplification direction. Our formulas of G are therefore not merely a matter of quantitative precision, but also important for a qualitative prediction.

Very recently, effort has been made to find OBC Green's function formulas from the conventional Brillouin zone [47]. Their results are applicable only to the simplest case where the hoppings exist only between nearest neighbors, in which case our results are consistent with theirs. It is highly challenging, if not impossible, to generalize their approach to the cases beyond nearest-neighbor hopping [e.g., our model Fig. 1(a)]. In contrast, our formulas are straightforward to use for general hoppings. Note that the necessity of taking OBC has been emphasized in recent insightful papers [46,47], though general formulas were lacking. In fact, if one takes PBC, the directional amplifiers become dynamically unstable,

which results from the endless amplification during the cyclic directional motion.

We note that our results are generalizable to more complicated boundary conditions such as domain wall geometries, for which GBZ remains definable [16]. Moreover, as the concept of GBZ also applies to higher dimensions [13,19], we expect that higher-dimensional generalizations of our formulas remain valid, though their applications rely on efficient algorithms of GBZ, which are called for in higher dimensions.

Realization in open quantum systems. So far, the non-Hermitian Hamiltonian is taken for granted. While it is without question in classical platforms, for example, the Green's function is directly measurable in the topolectrical circuits [6], we emphasize that our formulas are also applicable to various open quantum systems. For example, we may consider a 1D lattice of coupled bosonic modes, which can be realized in various realistic systems such as optomechanical cavities [38,54] and photonic lattices [43,55]. The bosonic modes are denoted by $a_1, \ldots, a_L$. For simplicity, let all modes have the same bare frequency ω_0, and each mode is coupled to its neighbors with strengths t_1 and t_2 [Fig. 1(d)]. Each site receives a coherent drive with amplitude $\epsilon_i(t)$, which can represent an incoming signal to be amplified. The Hamiltonian reads

$$H_0 = \sum_i [(t_1 a_i^\dagger a_{i+1} + t_2 a_i^\dagger a_{i+2} + \text{H.c.}) + \omega_0 a_i^\dagger a_i + \epsilon_i(t) a_i^\dagger + \epsilon_i^*(t) a_i]. \quad (12)$$

As the system is open, we consider the density matrix ρ, whose time evolution follows the quantum master equation

$$\dot{\rho}(t) = -i[H_0, \rho] + \sum_\mu \left(L_\mu \rho L_\mu^\dagger - \frac{1}{2}\{L_\mu^\dagger L_\mu, \rho\} \right), \quad (13)$$

where L_μ's are the dissipators describing the effects of environment. While the physics is general, we take the following set of dissipators for concreteness: $\{L_\mu\} = \{L_i^g, L_i^l\}$, including the single-particle gain $L_i^g = \sqrt{\gamma'} a_i^\dagger$ and loss $L_i^l = \sqrt{\gamma}(a_i - i a_{i+2})$. Feasible implementations of such dissipators have been discussed in detail [36,43].

The most measurable quantity is the field coherence $\psi_i(t) = \langle a_i(t) \rangle = \text{Tr}[a_i \rho(t)]$. It follows from Eq. (13) that they evolve under an effective non-Hermitian Hamiltonian H (see Supplemental Material [53]):

$$\dot{\psi}_i = -i \sum_j H_{ij} \psi_j - i\epsilon_i. \quad (14)$$

The same Eq. (14) also generally arises in other physical platforms of directional amplification. Our results will be independent of specific implementation and applicable to a general H. For the specific model in Fig. 1(d), H is found to be Fig. 1(a) (see Supplemental Material [53]) [56], with $\kappa = \frac{\gamma'}{2} - \gamma$.

Let us introduce the vector notation $\vec{\epsilon} = (\epsilon_1, \ldots, \epsilon_L)^T$, and similarly for $\vec{\psi}$. For a signal $\vec{\epsilon}$ with a frequency ω, $\vec{\epsilon}(t) = \vec{\epsilon}(\omega) \exp(-i\omega t)$, the resultant field is $\vec{\psi}(t) = \vec{\psi}(\omega) \exp(-i\omega t)$ whose amplitude is

$$\vec{\psi}(\omega) = G(\omega)\vec{\epsilon}(\omega), \quad G(\omega) = \frac{1}{\omega - H}. \quad (15)$$

To simplify notations, we shall measure the frequency with respect to ω_0, namely, rename $\omega - \omega_0$ as ω. Mathematically, this is equivalent to taking $\omega_0 = 0$. As such, negative ω denotes frequencies lower than ω_0.

It is now evident that the Green's function matrix G determines the amplification. For a signal entering the j site, with the only nonzero component of $\vec{\epsilon}$ being ϵ_j, the induced field at i site is $\psi_i(\omega) = G_{ij}(\omega)\epsilon_j(\omega)$. Note that, in the input-output formalism of amplification [57], the scattering matrix S is not exactly the same as, but has a simple relation to, the Green's function: $S_{ij}(\omega) = \delta_{ij} - i\mu_i\mu_j G_{ij}(\omega)$, with certain L-independent coefficients $\mu_{i,j}$ [37,46,47]. Therefore, S_{1L} (S_{L1}) is simply proportional to G_{1L} (G_{L1}), and it suffices to focus on G.

Discussions. We have obtained general formulas of the Green's function for 1D non-Hermitian systems. As a practical application, our results serve as simple formulas of the gain and directionality of directional amplification, which provide an efficient guide for designing high-quality directional amplifiers. The general applicability of our formulas is independent of the specific physical platform. Moreover, in view of the versatile roles of the Green's function in Hermitian systems, the general formula of the Green's function obtained here is expected to have various applications in non-Hermitian bands. For example, it will be useful in studying the interaction effects that are significant in many open hybrid systems.

Acknowledgments. We would like to thank H. Wang for helpful discussions. This work is supported by NSFC under Grant No. 11674189.

W.T.X., M.R.L., Y.M.H., and F.S. contributed equally to this work.

[1] S. Yao and Z. Wang, Edge States and Topological Invariants of Non-Hermitian Systems, Phys. Rev. Lett. **121**, 086803 (2018).

[2] F. K. Kunst, E. Edvardsson, J. C. Budich, and E. J. Bergholtz, Biorthogonal Bulk-Boundary Correspondence in Non-Hermitian Systems, Phys. Rev. Lett. **121**, 026808 (2018).

[3] C. H. Lee and R. Thomale, Anatomy of skin modes and topology in non-Hermitian systems, Phys. Rev. B **99**, 201103(R) (2019).

[4] V. M. Martinez Alvarez, J. E. Barrios Vargas, and L. E. F. Foa Torres, Non-Hermitian robust edge states in one dimension: Anomalous localization and eigenspace condensation at exceptional points, Phys. Rev. B **97**, 121401(R) (2018).

[5] L. Xiao, T. Deng, K. Wang, G. Zhu, Z. Wang, W. Yi, and P. Xue, Non-Hermitian bulk-boundary correspondence in quantum dynamics, Nat. Phys. **16**, 761 (2020).

[6] T. Helbig, T. Hofmann, S. Imhof, M. Abdelghany, T. Kiessling, L. W. Molenkamp, C. H. Lee, A. Szameit, M. Greiter, and R. Thomale, Generalized bulk–boundary correspondence in non-Hermitian topolectrical circuits, Nat. Phys. **16**, 747 (2020).

[7] A. Ghatak, M. Brandenbourger, J. van Wezel, and C. Coulais, Observation of non-Hermitian topology and its bulk–edge cor-

respondence in an active mechanical metamaterial, Proc. Natl. Acad. Sci. USA **117**, 29561 (2020).

[8] Our results will be generalizable to other boundary conditions such as domain wall systems. In mathematical literature, OBC corresponds to Toeplitz matrices, while PBC corresponds to circulant matrices.

[9] D. S. Borgnia, A. J. Kruchkov, and R.-J. Slager, Non-Hermitian Boundary Modes and Topology, Phys. Rev. Lett. **124**, 056802 (2020).

[10] H.-G. Zirnstein, G. Refael, and B. Rosenow, Bulk-Boundary Correspondence for Non-Hermitian Hamiltonians via Green Functions, Phys. Rev. Lett. **126**, 216407 (2021).

[11] M. G. Silveirinha, Topological theory of non-Hermitian photonic systems, Phys. Rev. B **99**, 125155 (2019).

[12] K. Yokomizo and S. Murakami, Non-Bloch Band Theory of Non-Hermitian Systems, Phys. Rev. Lett. **123**, 066404 (2019).

[13] S. Yao, F. Song, and Z. Wang, Non-Hermitian Chern Bands, Phys. Rev. Lett. **121**, 136802 (2018).

[14] S. Longhi, Probing non-Hermitian skin effect and non-Bloch phase transitions, Phys. Rev. Research **1**, 023013 (2019).

[15] Z. Yang, K. Zhang, C. Fang, and J. Hu, Non-Hermitian Bulk-Boundary Correspondence and Auxiliary Generalized Brillouin Zone Theory, Phys. Rev. Lett. **125**, 226402 (2020).

[16] T.-S. Deng and W. Yi, Non-Bloch topological invariants in a non-Hermitian domain wall system, Phys. Rev. B **100**, 035102 (2019).

[17] S. Longhi, Non-Bloch-Band Collapse and Chiral Zener Tunneling, Phys. Rev. Lett. **124**, 066602 (2020).

[18] K. Kawabata, N. Okuma, and M. Sato, Non-Bloch band theory of non-Hermitian Hamiltonians in the symplectic class, Phys. Rev. B **101**, 195147 (2020).

[19] T. Liu, Y.-R. Zhang, Q. Ai, Z. Gong, K. Kawabata, M. Ueda, and F. Nori, Second-Order Topological Phases in Non-Hermitian Systems, Phys. Rev. Lett. **122**, 076801 (2019).

[20] F. Song, S. Yao, and Z. Wang, Non-Hermitian Topological Invariants in Real Space, Phys. Rev. Lett. **123**, 246801 (2019).

[21] C. H. Lee, L. Li, R. Thomale, and J. Gong, Unraveling non-Hermitian pumping: Emergent spectral singularities and anomalous responses, Phys. Rev. B **102**, 085151 (2020).

[22] Y. Yi and Z. Yang, Non-Hermitian Skin Modes Induced by On-Site Dissipations and Chiral Tunneling Effect, Phys. Rev. Lett. **125**, 186802 (2020).

[23] E. J. Bergholtz, J. C. Budich, and F. K. Kunst, Exceptional topology of non-Hermitian systems, Rev. Mod. Phys. **93**, 015005 (2021).

[24] Y. Ashida, Z. Gong, and M. Ueda, Non-Hermitian physics, Adv. Phys. **69**, 249 (2020).

[25] B. Abdo, K. Sliwa, L. Frunzio, and M. Devoret, Directional Amplification with a Josephson Circuit, Phys. Rev. X **3**, 031001 (2013).

[26] B. Abdo, K. Sliwa, S. Shankar, M. Hatridge, L. Frunzio, R. Schoelkopf, and M. Devoret, Josephson Directional Amplifier for Quantum Measurement of Superconducting Circuits, Phys. Rev. Lett. **112**, 167701 (2014).

[27] K. M. Sliwa, M. Hatridge, A. Narla, S. Shankar, L. Frunzio, R. J. Schoelkopf, and M. H. Devoret, Reconfigurable Josephson Circulator/Directional Amplifier, Phys. Rev. X **5**, 041020 (2015).

[28] D. Jalas, A. Petrov, M. Eich, W. Freude, S. Fan, Z. Yu, R. Baets, M. Popović, A. Melloni, J. D. Joannopoulos *et al.*, What is—and what is not—an optical isolator, Nat. Photon. **7**, 579 (2013).

[29] L. Feng, M. Ayache, J. Huang, Y.-L. Xu, M.-H. Lu, Y.-F. Chen, Y. Fainman, and A. Scherer, Nonreciprocal light propagation in a silicon photonic circuit, Science **333**, 729 (2011).

[30] C. Caloz, A. Alù, S. Tretyakov, D. Sounas, K. Achouri, and Z.-L. Deck-Léger, Electromagnetic Nonreciprocity, Phys. Rev. Applied **10**, 047001 (2018).

[31] R. Fleury, D. L. Sounas, C. F. Sieck, M. R. Haberman, and A. Alù, Sound isolation and giant linear nonreciprocity in a compact acoustic circulator, Science **343**, 516 (2014).

[32] D. L. Sounas and A. Alù, Non-reciprocal photonics based on time modulation, Nat. Photon. **11**, 774 (2017).

[33] Z. Yu and S. Fan, Complete optical isolation created by indirect interband photonic transitions, Nat. Photon. **3**, 91 (2009).

[34] N. A. Estep, D. L. Sounas, J. Soric, and A. Alù, Magnetic-free non-reciprocity and isolation based on parametrically modulated coupled-resonator loops, Nat. Phys. **10**, 923 (2014).

[35] M. Soljačić, C. Luo, J. D. Joannopoulos, and S. Fan, Nonlinear photonic crystal microdevices for optical integration, Opt. Lett. **28**, 637 (2003).

[36] A. Metelmann and A. A. Clerk, Nonreciprocal Photon Transmission and Amplification via Reservoir Engineering, Phys. Rev. X **5**, 021025 (2015).

[37] L. Ranzani and J. Aumentado, Graph-based analysis of nonreciprocity in coupled-mode systems, New J. Phys. **17**, 023024 (2015).

[38] K. Fang, J. Luo, A. Metelmann, M. H. Matheny, F. Marquardt, A. A. Clerk, and O. Painter, Generalized non-reciprocity in an optomechanical circuit via synthetic magnetism and reservoir engineering, Nat. Phys. **13**, 465 (2017).

[39] S. Barzanjeh, M. Wulf, M. Peruzzo, M. Kalaee, P. Dieterle, O. Painter, and J. M. Fink, Mechanical on-chip microwave circulator, Nat. Commun. **8**, 953 (2017).

[40] G. A. Peterson, F. Lecocq, K. Cicak, R. W. Simmonds, J. Aumentado, and J. D. Teufel, Demonstration of Efficient Nonreciprocity in a Microwave Optomechanical Circuit, Phys. Rev. X **7**, 031001 (2017).

[41] N. R. Bernier, L. D. Toth, A Koottandavida, M. A. Ioannou, D. Malz, A. Nunnenkamp, A. K. Feofanov, and T. J. Kippenberg, Nonreciprocal reconfigurable microwave optomechanical circuit, Nat. Commun. **8**, 604 (2017).

[42] H Xu, L. Jiang, A. A. Clerk, and J. G. E. Harris, Nonreciprocal control and cooling of phonon modes in an optomechanical system, Nature (London) **568**, 65 (2019).

[43] D. Porras and S. Fernández-Lorenzo, Topological Amplification in Photonic Lattices, Phys. Rev. Lett. **122**, 143901 (2019).

[44] F. Ruesink, M.-A. Miri, A. Alu, and E. Verhagen, Nonreciprocity and magnetic-free isolation based on optomechanical interactions, Nat. Commun. **7**, 13662 (2016).

[45] S. Barzanjeh, M. Aquilina, and A. Xuereb, Manipulating the Flow of Thermal Noise in Quantum Devices, Phys. Rev. Lett. **120**, 060601 (2018).

[46] A. McDonald, T. Pereg-Barnea, and A. A. Clerk, Phase-Dependent Chiral Transport and Effective Non-Hermitian Dynamics in a Bosonic Kitaev-Majorana Chain, Phys. Rev. X **8**, 041031 (2018).

[47] C. C. Wanjura, M. Brunelli, and A. Nunnenkamp, Topological framework for directional amplification in driven-dissipative cavity arrays, Nat. Commun. **11**, 3149 (2020).

[48] Y.-P. Wang, J. W. Rao, Y. Yang, P.-C. Xu, Y. S. Gui, B. M. Yao, J. Q. You, and C.-M. Hu, Nonreciprocity and Unidirectional Invisibility in Cavity Magnonics, Phys. Rev. Lett. **123**, 127202 (2019).

[49] D. Malz, L. D. Tóth, N. R. Bernier, A. K. Feofanov, T. J. Kippenberg, and A. Nunnenkamp, Quantum-Limited Directional Amplifiers with Optomechanics, Phys. Rev. Lett. **120**, 023601 (2018).

[50] L. Mercier de Lépinay, E. Damskägg, C. F. Ockeloen-Korppi, and M. A. Sillanpää, Realization of Directional Amplification in a Microwave Optomechanical Device, Phys. Rev. Applied **11**, 034027 (2019).

[51] K. Zhang, Z. Yang, and C. Fang, Correspondence between Winding Numbers and Skin Modes in Non-Hermitian Systems, Phys. Rev. Lett. **125**, 126402 (2020).

[52] N. Okuma, K. Kawabata, K. Shiozaki, and M. Sato, Topological Origin of Non-Hermitian Skin Effects, Phys. Rev. Lett. **124**, 086801 (2020).

[53] See Supplemental Material at http://link.aps.org/supplemental/10.1103/PhysRevB.103.L241408 for the derivation of GBZ-based Green's function formulas, explicit expressions in terms of roots, multi-band models, and the derivation of non-Hermitian Hamiltonian from the quantum master equation.

[54] M. Aspelmeyer, T. J. Kippenberg, and F. Marquardt, Cavity optomechanics, Rev. Mod. Phys. **86**, 1391 (2014).

[55] M. Fitzpatrick, N. M. Sundaresan, A. C. Y. Li, J. Koch, and A. A. Houck, Observation of a Dissipative Phase Transition in a One-Dimensional Circuit QED Lattice, Phys. Rev. X **7**, 011016 (2017).

[56] It can be viewed as a boson counterpart of the fermion damping matrix [58].

[57] A. A. Clerk, M. H. Devoret, S. M. Girvin, F. Marquardt, and R. J. Schoelkopf, Introduction to quantum noise, measurement, and amplification, Rev. Mod. Phys. **82**, 1155 (2010).

[58] F. Song, S. Yao, and Z. Wang, Non-Hermitian Skin Effect and Chiral Damping in Open Quantum Systems, Phys. Rev. Lett. **123**, 170401 (2019).